

Final Draft
of the original manuscript:

da Conceicao, T.F.; Scharnagl, N.; Dietzel, W.; Kainer, K.U.:
**Corrosion Protection of Magnesium alloy AZ31 Sheets by Spin
Coating Process with Poly(ether imide) [PEI]**
In: Corrosion Science (2010) Elsevier

DOI: 10.1016/j.corsci.2010.02.027

Corrosion Protection of Magnesium alloy AZ31 Sheets by Spin Coating Process with Poly(ether imide) [PEI]

Thiago F. Conceicao¹, N. Scharnagl^{1,2}, C. Blawert¹, W. Dietzel¹, K.U. Kainer¹

¹Institute of Materials Research, GKSS-Forschungszentrum Geesthacht GmbH,
Max-Planck-Str. 1, D-21502 Geesthacht, Germany

²Berlin-Brandenburg Center for Regenerative Therapies - BCRT, Charité – Universitätsmedizin Berlin Campus Virchow
Klinikum, Augustenburger Platz 1, D-13353 Berlin, Germany

Abstract

In the present study, the potential of poly(ether imide) as corrosion protective coating for magnesium alloys was evaluated using the spin coating technique. The influence of different parameters on the coating properties was evaluated and the corrosion behaviour of the coatings was investigated using electrochemical impedance spectroscopy. The best corrosion protection was obtained preparing the coatings under N₂ atmosphere, using 15% wt. solution in N,N'- dimethylacetamide (DMAc) which resulted in a coating of approximately 2 μm thickness, with an initial impedance of 10⁹ Ω cm² and of 10⁵ Ω cm² after 240 h of exposure to a 3.5% NaCl solution.

Keywords: Poly(ether imide); Spin coating; Magnesium alloys; Corrosion.

1- Introduction

The application of polymeric layers on surfaces of metal sheets is a well known and interesting approach to inhibit metal corrosion [1,2]. As the corrosion of a metal surface is an electrochemical reaction between the metal and external agents (for example, oxygen and/or water) a polymeric layer can act as a barrier, preventing this reaction. Besides that, polymers combine properties like thermal, mechanical and chemical stability, depending on their structure and morphology, which yields a durable coating with longer life time of the protected metal [3,4].

The selection of the polymer for such a corrosion protection depends on both the metallic substrate and the polymer properties. In case of magnesium alloys which show severe corrosion in contact with water solutions containing Cl⁻ ions hydrophobic polymers are desirable. In this case, polymers with low oxygen permeability are not necessary, since the

corrosion rate of magnesium is independent of the oxygen concentration [5-8], different from iron and aluminium [7,8]. Besides the hydrophobic character, properties like thermal, mechanical and chemical stability, low water vapour permeability to avoid pressure increase due to hindered back-diffusion, good adhesion, good film forming properties and low ion permeability are important for a durable corrosion protective coating for magnesium alloys [3,4].

Due to their good mechanical properties, as high strength-to-weight ratio, magnesium alloys are promising light weight materials that are gaining application in many industrial sectors. The atmospheric corrosion properties of magnesium alloys are comparable to that of mild steel and are better than that of some aluminium alloys, due to the presence of a protective magnesium oxide/hydroxide film on the metal surface [9-11]. However, this protective film is unstable in aqueous solutions containing anions such as Cl^- and SO_4^{2-} , and the corrosion resistance of magnesium alloys under these conditions is extremely poor [6,8,11]. In the past it has been shown that the corrosion resistance of magnesium and its alloys in Cl^- solutions can be improved by acid treatment. This treatment removes impurities and can build protective compounds on the metal surface, such as MgF_2 which is formed by the HF treatment of magnesium and its alloys [12-15]. Nevertheless, the improvement on corrosion behaviour achieved by these treatments is not sufficient to provide long term protection of the metal in Cl^- containing environments.

As a hydrophobic thermal and mechanical stable polymer, poly(ether imide) (PEI) is a promising candidate for the corrosion protection of magnesium alloys. The potential of PEI coatings for this application was evaluated in a previous investigation of our group [16] where good degradation protection for Mg-alloys was achieved by PEI coatings prepared by the dip coating method, especially in the presence of inhibitors. This polymer class has satisfying film formation properties, which is one of the most critical points for the formation of a defect free coating, and is highly hydrophobic, as shown by Wang et al [17] using the precipitation value method. The literature also reports a water contact angle of 86° for PEI membranes [18], an intermediate value when compared to polyurethanes and polyesters used as coating for corrosion protection of aluminium [19,20] and PVDF films [21]. Besides that, poly(ether imide) can have a glass transition temperature higher than 200°C which provides a thermal stable coating at environmental conditions [22]. This is an important characteristic, since the literature reports a considerable decrease in the protective properties of coatings in temperatures above their T_g due to the increase of the diffusion coefficient of ions and water [23,24].

Another interesting characteristic of PEI is the presence of polar aromatic imide rings in the polymer structure which can enhance its adhesion on the metal substrate [25, 26]. According to studies in the literature, polymers with polar groups can behave as a base and oxides on the metal surface can behave as an acid, in the Lewis sense, and this acid-base interaction provides good adhesion between polymer and metal [3,25,26]. A good adhesion is not only important to maintain the coating on the metal, but it has also influence on the corrosion behaviour, as reported by Grundmeier et al [27], who showed that the corrosion protection of a coating depends more on the adhesion than on the diffusion of the corrosive specimens through the coating.

The deposition of a polymeric layer on the metal surface can be accomplished in different ways. Common coating processes used in industry are curtain coating [28,29], spray coating [30,31], dip coating [32,33] and spin coating [34,35]. In all these methods, the polymer is dissolved in an appropriate solvent, applied to the substrate and let to dry, or to cure in the case of thermosetting resins, until a solid film is formed. In this process, the type of solvent, solution concentration, application and drying procedures have significant influence on the final properties, including morphology, of the coating and consequently on the corrosion behaviour of the coated metal.

Among these methods, the spin coating offers advantages, such as thin and uniform thickness of the coating, low quantity of polymer needed in the solution, and fast evaporation of solvent, what makes this method very interesting for corrosion protection of magnesium alloys sheets. It consists of applying the polymer solution on the substrate surface and spinning it at a specific velocity. During the spinning process, the solution spreads over the substrate and the solvent evaporates, leaving a thin polymeric layer over the substrate surface. The aim of this study is to evaluate the corrosion behaviour of magnesium alloy AZ 31 sheets coated with PEI by spin coating process. The effect of solvent type, solution concentration, humidity and substrate pre-treatment on the coating properties was investigated, and the corrosion protection of the coatings was evaluated by impedance analyses.

2 – Experimental

2.1 – Materials

Magnesium alloy AZ31 sheets, with a chemical composition shown in Table 1 were used as substrate. Poly(ether imide) Ultem 1000[®] was obtained from General Electric and used without further purification. The solvents N,N'- dimethylacetamide (DMAc) and N-

methylpyrrolidone (NMP) of synthesis grade were obtained from Merck and used as received. Hydrofluoric acid (48% wt) and acetic acid (99% wt), used in the pre-treatment of the samples, were obtained from Aldrich and used as received.

2.2 – Substrate Pre-treatment

Three different pre-treatments were used to evaluate their effect on the coating properties: grinding, HF treatment and acetic acid cleaning. The grinding process consisted in grinding the samples with papers from 500 to 2500 grade, followed by degreasing using acetone. The HF treatment was performed as described in a previous study of the authors [12], using an HF concentration of 14 mol L^{-1} . In this treatment, besides the removal of iron, a thin layer of MgF_2 is deposited on the surface, which protects the metal from corrosion and enhances the adhesion of polymer coatings. The acetic acid cleaning consisted in dipping the samples in a 300 g L^{-1} solution of acetic acid in water, for 90 s. This cleaning process was selected based on the results reported by Nwaogu [36], who tested different acids for the cleaning of magnesium AZ31 alloy and reported high impurity removal with this kind of treatment.

2.3 – Solutions for the Coating Process

Solutions of PEI were prepared using DMAc and NMP as solvents, in the concentrations of 10 and 15% wt. These solvents and concentrations were selected due to promising results in previously spin coating tests. The viscosities of the solutions were measured using a Brookfield R/S-CPS rheometer at different shear rates. All the solutions showed a Newtonian behaviour.

2.4 – Coating Preparation

PEI coatings were prepared using a spin coater CeeTM 200 operated under room and N_2 atmosphere. Samples of dimensions 2 x 2 cm were spun at a specific velocity (1000 – 1600 rpm) during 100 s, when 3 mL of the polymer solution were applied to the substrate. After the coating step, the spin velocity was set to 3000 rpm during 150 s for the drying process. For samples coated under N_2 atmosphere using NMP as solvent, a second drying process was performed at 3500 rpm during 150 s. This second drying process was necessary

to ensure the dryness of the coating, which was not complete after the first one due to the low vapour pressure of NMP at room temperature. The drying of all samples was finalized by storing these under clean conditions for another 20 h at room temperature.

2.5 – Coating Characterisation

2.5.1 – Scanning Electron Microscopy (SEM) Analyses

As the coated samples had no surface conductivity, they were sputtered prior to the SEM analyses with gold by a passage of a current of 1.5 mA in a gold filament for 120 s. The morphologies of the surfaces were analyzed in a scanning electron microscope (SEM) Cambridge Stereoscan 200, using acceleration voltages from 3 to 10 kV, to obtain the best resolution.

2.5.2 – Fourier-transform Infrared Spectroscopy (FT-IR) Investigations

The presence of residual solvent on the coatings was analysed by FT-IR spectroscopy, using a Bruker Tensor 27 IR spectrometer. The surface was analysed by reflectance using an angle of 80 degree, from 300 cm^{-1} to 5000 cm^{-1} , with 2048 scans and 16k datapoints in a resolution of 4 cm^{-1} . The spectra were automatically converted to absorbance using the OPUS 6.5 (Bruker) software. To investigate eventual reactions between the polymer and corrosion products during the corrosion process, an IR microscope HYPERION 2000 was used in the visual-reflectance mode. The infrared spectra at specific points of the sample surface were recorded in a resolution of 4 cm^{-1} .

2.5.3 – Roughness and Thickness Measurements

The roughness of the coatings and substrates was measured using the profilometer Hommel Tester T100. For the thickness measurements, a coating piece close to the sample edges was removed using a sharp blade and the gap between coated and uncoated area was determined. The measured scanning distance was 4.8 mm.

2.5.4 – Adhesion Tests.

The wet adhesion of the coatings to the substrate which showed best performance was evaluated by pull-off test performed on a PosiTest Pull-OFF Adhesion Tester from DeFelsko, in accordance with ASTM D 4541 and ISO 4624. The tests were performed in the wet condition due to its higher significance in the coating performance than the dried one, according to studies in the literature [37]. A dolly of 20mm size was adhered to the coating surface using Alderite adhesive which was cured at 60 °C for 2 h. The samples were then immersed in distilled water for 24 h at room temperature. After immersion, the dolly was connected to the actuator of a hydraulic pump and the strength necessary to pull off the coatings was measured within a resolution of 0.01 MPa. Three to five measurements were performed for each sample.

2.6 - Electrochemical Impedance Spectroscopy (EIS).

The corrosion behaviour of the samples was evaluated in a three electrode cell, where the sample, a platinum mesh and an Ag/AgCl electrode were the working, the counter and the reference electrode, respectively. A sample area of 1.54 cm² was exposed to a 3.5% NaCl solution, and the impedance of the samples was measured at different exposure time. As the current through an insulator polymeric layer is extremely low, the cell was connected to a Femto Amp device, which increases the low current detection capacity. The whole cell was placed inside a faraday cage to avoid Coulombs fields and was connected to a potentiostat Gill AC from ACM instruments. The open circuit potential was measured for 15 min and then the impedance test was carried out at open circuit potential by applying a sinusoidal potential in frequencies from 10⁴ Hz to 10⁻² Hz, with amplitude of 15 mV. The impedance behaviour of selected samples was simulated using the software Zview2 to study their degradation mechanism.

3- Results and Discussion

3.1- Morphology and Thickness

The spin coating process is a useful and common tool for the preparation of extreme thin and uniform films on flat substrates. This coating method is used in electronics industry,

e.g. wafer coating, and for the preparation of solid oxide fuel cells (SOFC) [38-41]. One of the main advantages of this method is the thickness uniformity of the prepared coating, which is a problem for other coatings methods, as dip coating, where the solvent flow induces non uniform covering of the surface, and consequently defect formation [42]. Besides that, the thickness of the coatings can be controlled by spin speed and solution concentration, what allows the formation of uniform coatings with specific thicknesses. As a drawback, this method is restricted to flat substrates and it is not suited for large production rates since it is a batch process [42].

The morphology of PEI coatings prepared by spin coating is extremely influenced by atmospheric humidity, as can be seen in Figure 1. Under standard room conditions with certain humidity, the coatings had a white appearance indicating a porous morphology, as could be confirmed by the SEM images shown in Figures 2a and 2c. These pores, with *ca* 2 μm of diameter, are formed due to the polymer precipitation in presence of air humidity [16, 43]. A similar behaviour is reported by Eisenbraun [34, 35] for polyamic acid and fluorinated polyimide. Under N_2 atmosphere, the dry gas induces a phase inversion process governed by solvent evaporation, what leads to a transparent, non-porous coating, as can be observed in Figures 2b and 2d.

The thickness of the coatings varied with spin speed, atmosphere, solution concentration and solvent type as shown in Figure 3. For all the conditions, the thickness decreases with the spin speed, due to the increase in the centrifugal force acting on the solution. A higher centrifugal force results in a higher solution outflow from the substrate, thinning the film. The influence of the atmosphere can be observed by comparing figures 3a with 3b. The higher thickness obtained at room atmosphere is related to the faster rate of polymer precipitation, induced by air humidity, than of solvent evaporation under N_2 atmosphere. After the polymer precipitation, the film could not undergo a further thinning process, and hence, the thickness at this condition was higher. The effect of humidity on the polymer precipitation was stronger for PEI/DMAc (10/90) than for PEI/NMP (10/90), as observed during the coating process, and for this reason, the former one resulted in thicker coatings. Solutions of 15% wt were not used at room conditions due to non uniform covering of the substrate, as observed in previous tests. This is probably related to a very high polymer precipitation rate of this solution at room atmosphere which inhibited the formation of a uniform layer.

The influence of the solution concentration on the coating thickness, observed for the coatings prepared under N_2 atmosphere, Figure 3b, is associated with the solution viscosity. According to studies in the literature, for the same solute solvent system and the same spin

speed [44-47], the higher the viscosity the thicker the film, due to the lower outflow of a more viscous solution. As shown in Table 2, the 15% wt solutions had higher viscosities than the 10% wt solutions, and for that reason, produced thicker coatings.

Despite the lower initial viscosity of the solution PEI/DMAc (15/85) compared to PEI/NMP (15/85), shown in Table 2, the first one produced thicker coatings. This result is related to the solvent evaporation during the spin coating process, which leads to a viscosity increase [48]. As shown in Table 2, DMAc has a much lower boiling point than NMP, being more volatile. Hence, at the beginning of the spin coating process, PEI/DMAc (15/85) undergoes a higher viscosity increase than PEI/NMP (15/85), due to its higher solvent evaporation rate. Due to this viscosity increase, PEI/DMAc (15/85) produces thicker coatings. This result is in agreement with that of Yimsiri et. al [47], who showed that, when the solvent evaporation was significant, the initial viscosity of the solution did not play a significant role in the coating thickness. Besides that, the extra drying process applied on the samples coated using NMP solutions produces a further thinning in these coatings.

3.2 – EIS and FTIR Investigations

Figure 4 shows the impedance spectra of samples spin coated under room and N₂ atmosphere. The impedance of the samples coated with PEI/DMAc (10/90) at room conditions, Figure 4a, is in the order of 10⁵ Ω cm², in the same magnitude of PEO coatings described in the literature [49-51], and only one order of magnitude lower than the coatings prepared under N₂ atmosphere, Figure 4b. Nevertheless, despite this considerably high initial impedance, the coatings prepared at room atmosphere did not show good protective properties at longer exposure times to the corrosive solution, and the coatings morphology was highly sensitive to humidity variations, what affected the reproducibility of the results. For this reason, further characterization was focused on coatings prepared under N₂ atmosphere.

Due to the non-porous morphology of the samples prepared under N₂ atmosphere, these showed good corrosion protection after longer exposure time to the corrosive solution. Figure 5 shows the impedance variation with time of coatings prepared using DMAc as solvent. The decrease in the impedance with the exposure time indicates the diffusion of water and ions through the coating which increased its dielectric constant, and consequently, decreased its resistance [3,27]. After 20 h of exposure to the corrosive solution, the samples spin-coated with PEI/DMAc (10/90), Figure 5a, showed impedances in the order of 10⁴ Ω cm² and a capacitive behaviour in a small frequency range (10³ - 10⁴ Hz) indicating that the coating

considerably had lost its capacity to separate the solution from the metallic substrate [3,27,52]. After 48 h of exposure, this coating was completely degraded

The samples coated using PEI/DMAc (15/85), Figure 5b, showed better result due to their higher thickness. The initial impedance in the order of $10^9 \Omega \text{ cm}^2$, in the same order of PEI coatings prepared by dip coating using CH_2Cl_2 as solvent, reported in a previous publication of our group [16]. At 72 h of exposure the spectra started to change in frequencies below 10^0 Hz , showing another capacitive part, indicating the gradual concentration of water and anions on the metal/polymer interface. According to Grundmeier [27], this second capacitive part is related to a double layer of ions at the metal/coating interface, and indicates delamination of the coating. At this exposure time, the impedance dropped to $10^7 \Omega \text{ cm}^2$ and maintained this value for the next 192 h, what is an excellent result for coated magnesium compounds compared to other reports in the literature [49-51, 53]. Three measurements were performed for this sample, and all showed a similar behaviour. At 240 h of exposure, the sample coated with PEI/DMAc (15/85) showed impedance in the order of $10^5 \Omega \text{ cm}^2$ which is the highest impedance after such a long exposure time for a polymer coated magnesium alloy that came to the authors knowledge. The impedance considerably dropped 24 h after that, reaching values of the uncoated metal.

The samples coated with PEI/NMP (10/90), Figure 6a, showed impedance values of $10^4 \Omega \text{ cm}^2$ after only 4 h of exposure, indicating that the solution could easily penetrate the coating and reach the substrate. This could be confirmed by a second capacitive behaviour that appeared after 1h of exposure in the frequency range of 10^0 – 10^2 Hz , which is related to a double layer of ions on the metal surface [3, 27]. After 10 h of exposure, the coatings prepared using PEI/NMP (10/90) showed considerable degradation. The samples coated using PEI/NMP (15/85) did not have the same behaviour as those coated using PEI/DMAc (15/85) and showed considerable degradation after 48 h of exposure (Figure 6b). The reason for the inferior behaviour of the coatings prepared using NMP in both concentrations is related to residual solvent and, in the case of coatings prepared using 15% wt solution, to their lower thickness.

Figure 7 shows the FTIR spectra of coatings prepared using NMP and DMAc as solvents, before and after drying in a vacuum oven at 135° C during 12 h. In Figure 7a the vanishing of the signals indicated by the arrows after the drying process can be observed, which are related to NMP. Figure 7a also shows the influence of the solvent on the signal around 1360 cm^{-1} which is related to the C-N-C stretching mode of the imide ring [54]. This signal usually appears centred at 1365 cm^{-1} with a small shoulder around 1380 cm^{-1} , as it

appears in Figure 7b, but in the coating prepared using NMP this signal splits in three. This suggests that NMP strongly interacts with the imide ring of PEI, what makes it difficult to remove by spin coating even after the drying in the vacuum oven, as the signal around 1360 cm^{-1} still indicates residual amounts of NMP. Figure 7b shows that the coatings prepared using DMAc also contained residual solvent, but this could be eliminated after drying in the oven and did not show interactions with the imide ring.

However, thermo gravimetric analyses showed an equal amount of solvent for both coatings, of approx. 6 % in weight. Therefore, it seems that the influence of residual solvent is not related to different quantities on the two systems (NMP and DMAc) but rather to different interactions between solvent and polymer. It is possible that NMP plasticizes the polymer inducing a T_g decrease and a consequently increase in the diffusion of corrosive specimens through the coating [2]. However the T_g of the PEI-NMP pair could not be determined by thermal analyses since that the T_g of pure PEI is in the same temperature range of the boiling point of NMP. Other analysis as dynamic mechanical thermal analyse will be performed to confirm this.

3.3- Substrate Pre-treatment

Figure 8 shows the pre-treatment effect on the coatings morphology. The pre-treatment is an important process for the corrosion protection of coatings, since it influences the adhesion, the film formation process and the impurities concentration on the metal surface. It can be observed that the coatings prepared over acid treated substrates have a non uniform morphology. This is due to the surface roughness effects, as shown in Table 3. The acetic acid treatment resulted in a higher increase in surface roughness (from $0.09\text{ }\mu\text{m}$ to $2.21\text{ }\mu\text{m}$) than the HF one (from $0.09\text{ }\mu\text{m}$ to $0.37\text{ }\mu\text{m}$), due to a higher dissolution rate of the metal [36]. This higher substrate surface roughness induces a higher coating surface roughness, as can be observed in Figure 8a and Table 3.

The lower surface roughness increase obtained by the HF treatment is related to a lower metal dissolution rate, which takes place at the very beginning of the treatment, and to the lower protective layer deposition rate, which takes place during the treatment [12]. These lower rates allow a more uniform modification of the surface, compared to the acetic acid treatment, which allow the formation of a more uniform coating, as can be observed in Figure 8b and Table 3. Nevertheless, both acid treatments produced rougher surfaces compared to the

grinding process, which allow the formation of a smooth coating with a surface roughness of 0.03 μm (Figure 8c).

These coating morphologies have direct influence on their protective properties, as can be seen in Figure 9, where the low frequency impedance of HF-treated and acetic acid cleaned samples are shown. Comparing the values in Figure 9 related to coatings prepared using PEI/DMAc (15/85) with Figure 5b, it can be observed that the coated HF-treated samples have a lower impedance than the grinded ones. After 96h of exposure, they showed impedances close to that of uncoated substrate, in the order of $10^5 \Omega \text{ cm}^2$, while the coated grinded substrates showed such impedance only after 240 h of exposure. For the HF-treated substrates coated using PEI/NMP (15/85), the impedance was close to that of the uncoated substrate after 20 h of exposure, and after 48 h, the impedance was even lower, showing that the substrate started to degrade. This is an interesting result compared to a previous study of our group [12], where it was shown that the HF pre-treatment improved the corrosion behaviour of PEI coatings prepared by the dip coating method. This difference is related to the thickness of the coatings. The dip coating method produced coatings with a thickness of *ca* 10 μm , thick enough to cover the irregularities produced by the HF treated substrate. Nevertheless, as the spin coating method produces very thin coatings, the substrate has to be smooth to avoid defects on the coating.

The coatings prepared on acetic acid cleaned substrate showed the worse corrosion behaviour. Despite the impurities removal [36] this treatment resulted in a significant surface roughness increase, as previously commented, which results in very low impedance. Nevertheless, this roughness effect can be minimized by the use of increased coating thickness, and this cleaning process can be an interesting pre-treatment when other coatings methods which produce thicker coatings are applied.

3.4 – Investigations on the Mechanism of Coating Degradation

3.4.1 – EIS Simulations and Adhesion Tests

The mechanism of coating degradation was studied in details using electronic circuit modelling. This is a powerful tool which gives insights on the permeability of corrosive specimens in the coating and has been used by many researchers to elucidate the corrosion mechanism of coated metals [27, 49-51, 55, 56]. In Figure 10a can be observed the fitting result for the theta Bode plot of the sample which showed the best behaviour in EIS tests,

PEI/DMAc (15/85) prepared over grinded substrates. The circuit model used in this fitting process is shown in Figure 10b, and it can be seen from Figure 10a that it simulates very well the electrochemical behaviour of this sample.

This circuit differs from the main circuit used for simulation of coated metals [27,55] by an extra constant phase element (CPE) in parallel with other resistance, which is here called CPE₁ and R₁. As described by many authors, CPE is an element that permits the simulation of phenomena that deviates from a pure capacitive behaviour, and its impedance can be mathematically defined as:

$$Z = (j\omega)^{-P}/T \quad \text{equation 1}$$

where Z is the impedance, j the imaginary number, ω the angular frequency, T and P are constants of the CPE. When P is equal to 1, the CPE behaves as a pure capacitor, when P is equal to 0 it represents a resistor and when it is equal to -1 represents an inductor. As can be observed in Table 4, for CPE₁ and CPE₂ the value of P is very close to 1 and they behave similarly as pure capacitors.

The addition of CPE₁ and R₁ in parallel was necessary to correctly simulate the behaviour observed in Figure 10a. At high frequencies, the theta shows two distinct loops, which are observed in all the immersion times (240 h is the only exception). At certain exposure times, the theta Bode plot clearly shows three time constants, what was impossible to simulate using the traditional two CPEs circuit. CPE₁ and R₁ are related to solvent-rich domains while CPE₂ and R₂ are related to solvent-poor domains. As previously reported these coatings have residual solvent of approx. 6% weight that can be located at specific domains. The diffusion of electrolytes will be higher in the solvent-rich domain than in the solvent-poor one leading to different electrolyte contents, and this different electrolyte content results in distinct values of the CPE constants. This can be better understood evaluating the expression of capacitance in terms of dielectric constant and film dimensions:

$$C = \epsilon \epsilon_0 A/d \quad \text{equation 2}$$

where C is the capacitance, ϵ is the relative dielectric constant of the material, ϵ_0 is the dielectric constant in vacuum, A is the area and d the thickness. As CPE₁ and CPE₂ are very similar to pure capacitors (P close to 1), their T constant follows the same trend as the capacitance in equation 2, being directly proportional to dielectric properties and area and

inversely proportional to the thickness. In this way, different electrolyte contents results in different dielectric constants and distinct values of T . Therefore, the correct evaluation of this coating performance must take into account the different contributions of solvent-rich and solvent-poor domains to the dielectric property of the coating.

The relation between CPE_1 with solvent-rich domains could be confirmed by the EIS spectrum of a sample dried in a vacuum oven, as shown in Figure 11. It can be observed that the time constant at high frequencies, present in the spectra of spin coated samples, vanishes when the sample is dried in the oven. In this paper we are interested in evaluate the behavior of coatings prepared by spin coating without further heat treatment to show the potential of this simple process for the preparation of protective coatings. Therefore, only the mechanism of spin coated samples without further heat treatment will be investigated.

It can be observed in Table 4 that T_1 maintains a constant value in the first 3h of exposure, show a slightly increase after 72 h and decreases after 144 h while T_2 shows a progressive increase during the whole exposure time. This constant value of T_1 in the beginning of exposure suggests that the solvent-rich domains on the coating surface are saturated with electrolytes. At this saturation stage, when an electrolyte enters in the solvent-rich domain of the coating an equal amount goes from it to the solution and/or to the solvent-poor domain inducing an increase in T_2 and a constant value of T_1 . Considering that the solvent-rich domains on the coating surface are saturated, the following variations in T_1 are entirely related to changes in the A/d ratio of equation 2. The increase in T_1 observed until 72 h suggests that the electrolytes diffuses in the film and reaches others solvent-rich domains, increasing the area of saturated solvent-rich domains, and consequently, producing an increase in T_1 . This is schematically shown in Figure 12.

After certain exposure time the solvent-rich domains will be saturated in the entire coating exposed area (case 2 in Figure 12) and the following variations in T_1 will be entirely related to changes in thickness. As the electrolytes get deep into the coatings, the total thickness of the saturated solvent-rich domains (the summation of the thicknesses of all the separated saturated solvent-rich domains) increases, leading to the decrease in T_1 that is observed at 144 h. On the other hand, the value of T_2 increases constantly during the whole exposure time due to the increase in dielectric constant produced by the flux of electrolytes from the solution and saturated solvent-rich domain to the solvent-poor domain.

This model predicts that after certain exposure time, all the solvent-rich domains will be saturated with electrolytes in the whole volume of the exposed coating and T_1 will be constant. At this time, electrolytes will diffuse from the solvent-rich domain to the solvent-

poor one until they have the same electrolyte content, and CPE_1 and CPE_2 will merge in one single CPE. This is confirmed by the curve of 240 h of exposure in Figure 10a where only one time constant can be observed at high frequencies, indicating an equal electrolyte distribution in the coating. This curve was simulated using the traditional two CPE circuit (without CPE_1 and R_1) and it can be observed from Figure 10a and Table 4 that the model fitted very well in the curve and that the values follow the trend observed in the other exposure times.

Interesting considerations can also be done regarding R_1 and R_2 . Table 4 shows that R_1 increase while R_2 decreases during all exposure times. The decrease of R_2 is a normal and expected behaviour related to the increase in the electrolyte content in the solvent-poor domain. In the case of R_1 , the increase can be related to solvent been washed out from the coating. When the solvent is washed out, the resistance of the solvent-rich domain moves towards the resistance of the solvent-poor domain. However, as the increase was small compared to R_2 , it can be conclude that only a small amount of solvent was washed out until 144 h of exposure. It is interesting to observe that R_2 is three orders of magnitude higher than R_1 at the first hours of exposure, but after 144 h, they are in similar order of magnitude. This is another indicative that the electrolytic distribution becomes more homogeneous with the exposure time, and that the differences in electrolytes contents between solvent-rich and solvent-poor domains becomes smaller until only one CPE is observed.

Besides this two coatings constant phase elements, a third one related to the double layer of ions in the polymer-metal interface is observed. This double layer CPE appears even after 15min of exposure, suggesting the presence of small defects in the coating which allowed the fast arrival of electrolytes in the interface. As expected, T_{dl} increases and R_{ct} decreases with exposure time, indicating the increase of electrolyte in the interface.

The behaviour of samples coated using PEI/NMP (15/85) follow similar trend as the one described above, as shown in Figure 10c. It also shows two different constant related to solvent-rich and solvent-poor domains that could be simulated using the circuit shown in Figure 10b. T_1 maintain a constant value during 10 h and show a decrease after that, while T_2 shows a constant increase (Table 5). This decrease in T_1 after 10 h shows that the electrolytes could easily penetrate the coating causing the increase in thickness of saturated solvent-rich domains, as discussed above. It is also interesting to note that the value of T_2 almost quadruplicate in 24 h of exposure, indicating a fast diffusion of ions in the coating. Such high increase was not observed for the coatings prepared using DMAc even after 144 h, what shows that the electrolytes had a much higher diffusion in the coatings prepared using NMP

than in the ones prepared using DMAc. This higher diffusion is associated to the stronger interaction between NMP and the polymer, as previously commented.

Similarly to the coatings prepared using DMAc, R_1 increases while R_2 decreases. However, the difference in R_1 and R_2 is not so pronounced in this coating as it is in the one prepared using DMAc. This suggests that the solvent is more uniformly distributed in this coating, what is in agreement with the stronger interaction in the PEI-NMP pair than in the PEI-DMAc one. At 48 h of exposure, the behaviour of this coating is similar to the uncoated metal, as shown in Figure 6b, showing that the coating had completely degraded.

Besides the simulation of the impedance spectra of the coatings, their wet adhesion was measured to evaluate its effects on the corrosion protection. Table 6 shows that the adhesion was similar for the samples prepared using DMAc and NMP as solvents, with a value of approximately 2 MPa, in the same range of some epoxy coatings described in the literature for the corrosion protection of aluminium alloys [57]. These results shows that the rate determining effect of the impedance decrease with exposure time is not adhesion loss, but rather the difference in electrolytes diffusion trough the coating. The higher electrolyte diffusion through the coatings prepared using NMP allow higher currents trough the coating that decreases its impedance. Therefore, considering the spin coating method without further drying steps, the solution PEI/DMAc (15/85) produces more protective coatings than PEI/NMP (15/85) due to its higher thickness and lower electrolyte diffusion rates.

3.4.2 – FTIR Microscopy Investigations

To investigate whether any reaction between the polymer and the corrosion products took place during the corrosion of the samples (especially the possible opening of PEI imide ring by $Mg(OH)_2$), IR microscopy was used. This investigation is important for a better understanding of the mechanism of coating degradation. Figure 13a shows the microscopic view of a sample spin-coated with PEI/DMAc (10/90) after the corrosion test, where an undamaged and damaged area can be seen. The IR spectra of these areas, Figure 13b, reveal the presence of O-H signals on the damaged area, which are related to magnesium hydroxide. The sharp signal at 3700 cm^{-1} is related to brucite crystals ($Mg(OH)_2$) which do not form hydrogen bonds [50] The broad signals in the range from 3000 and 3500 cm^{-1} are related to magnesium hydroxide forming hydrogen bonds and probably to crystallization water [58-60] The signals that appeared in the range of 1400 to 1600 cm^{-1} on the damaged area are related to magnesium compounds like Mg_2CO_3 [58]

To evaluate whether the ring opening reaction took place, the ratio of the signal related to the carbonyl group and the one related to the ether linkage (Ar-O-Ar) of the PEI structure, were investigated for the damaged and undamaged areas. Very small or no variation was observed, suggesting that the polymer was not affected by any corrosion product. However, it is possible that the signals related to the polyamic acid (opened imide ring) were not visible as their intensity might be too low to be detected by FTIR-spectroscopy in relation to the PEI-signals. Therefore, the ring-opening reaction might have occurred but its relevance is still unclear. It seems that the main factor related to the coating degradation is the bursting of the coating due to the formation of corrosion products. As can be seen in Figure 12b, the signals related to corrosion products are much more intense than those related to the polymer on the damaged area, indicating that the polymer coating was removed on the areas of corrosion. The higher degradation rate of the samples prepared using NMP is therefore associated with the higher electrolyte diffusion rate through the coating that causes higher passage of current resulting in more corrosion products forming in the interface and bursting of the coating.

4 – Conclusions

Protective coatings of PEI were successfully applied to the surface of magnesium AZ31 alloy by a spin coating process. The coatings showed significant influence of atmospheric humidity, having a porous morphology when prepared under room conditions, and a dense one when prepared under N₂ atmosphere. The maximum thickness was 3.2 μm, produced by the solution PEI/DMAc (15/85) at the spin speed of 1000 rpm. The solvents had significant effect on the coatings performance. The coatings prepared using DMAc showed better corrosion protection than those prepared using NMP in both concentrations (10 % and 15% wt). This is due to the lower rate of diffusion of corrosive specimens and to the higher thickness, in the case of 15% wt solutions.

The optimized conditions for the preparation of corrosion protection PEI coatings by the spin coating method is performing the coating under N₂ atmosphere at 1000-1400 rpm, using the solution PEI/DMAc (15/85) and grinded substrates. These coatings showed initial impedances in the order of 10⁹ Ω cm² and impedances in the order of 10⁵ Ω cm² after 240 h of exposure to the corrosive solution. EIS simulation results showed that the diffusion of electrolytes in the coating starts in solvent-rich domains and spread in the coatings through them. The initial high frequency behavior of the coating must be simulated considering two different CPEs, related to solvent-rich and solvent-poor domains. The results showed a higher

electrolyte diffusion rate in the coatings prepared using NMP than in the ones prepared using DMAc. The coatings adhesion was not influenced by the used solvent.

The acid treatments were not beneficial to the performance of the coatings, since they produced irregular surfaces which interfered in the formation of a defect free coating. The HF pre-treatment showed better results than the acetic acid cleaning due to the lower surface roughness increase. The results show the good potential of PEI for corrosion protective coatings, with high impedance at thin thickness. Nevertheless, other pre-treatments for the preparation of these coatings by spin coating should be investigated, since the grinding process is not suitable for industrial application and the used chemical pre-treatments showed inferior properties than the grinding.

5 – References

- [1] P.R. Khaladkar, Uhlig's Corrosion Handbook, 2nd Edition, John Wiley & Sons, INC. 2000, 965.
- [2] C.H. Hare, Uhlig's Corrosion Handbook, 2nd Edition, John Wiley & Sons, INC. 2000, 1023.
- [3] G. Grundmeier, A. Simoes, Encyclopedia of Electrochemistry, Ed. Allen Bard and Martin Stratmann; Vol.4, Wiley-VCH Verlag GmbH, Weinheim, 2003, 500.
- [4] J.E. Gray, B. Luan, J. Alloys Compd. 336 (2002) 88.
- [5] G. Baril, N. Pebere, Corros. Sci. 43 (2001) 471.
- [6] A. Pardo, M.C. Merino, A.E. Coy, R. Arrabal, F. Viejo, E. Matykina, Corros. Sci. 50 (2008) 823.
- [7] L.L. Shreir, R.A. Jarman, G.T. Burstein, Corrosion: Metal/Environmental reactions, 3th Ed, Butterworth-Heinemann, 1994
- [8] R.W. Revie, Uhlig's Corrosion Handbook, 2nd Edition, John Wiley & Sons, INC. 2000.
- [9] K.N. Reichek, K.J. Clark, J. E Hilis, SAE Technical Paper Series 850417, Detroit 1985
- [10] J.F. King, Adv. Eng. Mater. Techno. Int., Sterling, London 1990.
- [11] G. Ling, A. Atrens, Adv. Eng. Mater. 1 (1999) 11.
- [12] T.F. Conceicao, N. Scharnagl, C. Blawert, W. Dietzel, K.U. Kainer, Thin Solid Films, submitted paper.
- [13] H.H. Elsentriecy, K. Azumi, H.Konno, Surf. Coat. Technol.202 (2007) 2007.

- [14] R. Suplit, T. Koch, U. Schubert, *Corros. Sci.* 49 (2007) 3015.
- [15] K.Y. Chiu, M.H. Wong, F.T. Cheng, H.C. Man, *Surf. Coat. Technol.* 202 (2007) 590.
- [16] N. Scharnagl, C. Blawert, W. Dietzel, *Surf. Coat. Technol.* 203 (2009) 1423.
- [17] D. Wang, K. Li, W.K. Teo, *J. Appl. Polym. Sci.* 71 (1999) 1789.
- [18] M. Khayet, *Appl. Surf. Sci.* 238 (2004) 269
- [19] S.S. Pathak, A. Sharma, A.S. Khanna, *Prog. Org. Coat.* 65 (2009) 206.
- [20] S.S. Pathak, A.S. Khanna, *Prog. Org. Coat.* 65 (2009) 288.
- [21] B.B.J. Basu, A.K. Paranthaman, *Appl. Surf. Sci.* 255 (2009) 4479.
- [22] J. Brandrup, E.H. Immergut, E.A. Grulke, *Polymer Handbook*, fourth edition, John Wiley and Sons, 1999.
- [23] J. Li, C.S. Jeffcoate, G.P. Bierwagen, D.J. Mills, D.E. Tallman, *Corrosion*, 54 (1998) 763.
- [24] G. Bierwagen, *J. Coat. Technol.* 5 (2008) 133.
- [25] M. Grujicic, V. Sellappan, M.A. Omar, N. Seyr, A. Obieglo, M. Erdmann, J. Holzleitner, *J. Mater. Process. Technol.* 197(2008) 363.
- [26] F.M. Fowkes, Sun Cy, S.T. Joslin, *Corrosion control by Organic Coatings*, Ed Leidheiser Jr, NACE International Huston.
- [27] G. Grundmeier, W. Schmidt, W. Stratmann, *Electrochim. Acta*, 45 (2000) 2515.
- [28] D.R. Brown, *J. Fluid Mech.* 10 (1961) 297.
- [29] Ridley, US Patent 4019906.
- [30] Murayama, US Patent 4977000.
- [31] D.A. Ansdell, *Paint and Surface Coatings* (Edited by R Lambourne) Ch 10, Halsted Press, New York (1987).
- [32] Nakashima, US Patent 4353934.
- [33] Bell, US Patent 6451383.
- [34] Eisenbraun, US Patent 4996254.
- [35] Eisenbraun, US Patent 4997869.
- [36] U. C. Nwaogu, A thesis report on the effects of cleaning processes on the corrosion behaviour of magnesium alloy sheet, Master Thesis, Joint European Masters in Materials Science, Institute of materials research, GKSS Forschungszentrum, 2008.
- [37] Funke W, *Prog. Org. Coat.* 28 (1996) 3
- [38] W.W. Flack, D.S. Soong, A.T. Bell, D.W. Hess, *J. Appl. Phys.* 56, (1984) 1199.
- [39] S.A. Jenekhe, S.B. Schuldt, *Ind. Eng. Chem. Fundam.* 23 (1984) 432.

- [40] Jasinski P, Molin S, Gazda M, Petrovskyc V, Anderson H U, J. Power Sources, 194 (2009) 10.
- [41] K. Chena, Y. Tiana, Z. Lüa, N. Aia, X. Huanga, W.Su, J. Power Sources, 186 (2009) 128.
- [42] G.P. Bierwagen, Electrochim. Acta, 37 (1992) 1471.
- [43] M. Mulder, Basic Principles of Membrane Technology, Kluwer Academic Publishers, Netherlands, 1991.
- [44] W.A. Levinson, A. Arnold, O. Dehodgins, Poly. Eng. Sci, 33 (1993) 980.
- [45] S.A. Jenekhe, Poly. Eng. Sci, 23 (1983) 830.
- [46] C.W. Extrand, Poly. Eng. Sci, 34 (1994) 390.
- [47] P.Yimsiri, M.R. Mackley, Chem. Eng. Sci. 61 (2001) 3496.
- [48] K.J. Skrobis, D.D. Denton, A.V. Skrobis, Poly. Eng. Sci. 30 (1990) 193.
- [49] A. Ghasemi, V.S. Raja, C. Blawert, W. Dietzel, K.U. Kainer, Surf. Coat. Technol. 202 (2008) 3513.
- [50] P.B. Srinivasan, J. Liang, C. Blawert, M. Störmer, W. Dietzel, Appl. Surf. Sci. 255 (2009) 4212.
- [51] P.B. Srinivasan, C. Blawert, W. Dietzel, Mater. Sci. Eng., A 494 (2008) 401.
- [52] J. Titz, G.H. Wagner, H. Spähn, M. Ebert, K. Jüttner, W.J. Lorenz, Corrosion, 46 (1989) 221.
- [53] M.B. Kannan, D. Gomes, W. Dietzel, V. Abetz, Surf. Coat. Technol. 202 (2008) 4598.
- [54] J. Kurdi, A. Kumar, Polymer, 46 (2005) 6910.
- [55] Zhang J, Hu J, Zhang J, Cao C, Prog. Org. Coat. 51 (2004) 145.
- [56] Deflorian F, Fedrizzi L, Lenti D, Bonora P L, Prog. Org. Coat. 22 (1993) 39.
- [57] Mohseni M, Mirabedini M, Hashemi M, Thompson G E, Prog. Org. Coat. 57 (2006) 307.
- [58] Jönsen M, Persson D, Thierry D, Corros. Sci. 49 (2007) 1540.
- [59] J.T. Kloprogge, L. Hickey, R.L. Frost, J Raman Spectr. 35 (2004) 967.
- [60] B. Karmakar, P. Kundu, R.N. Dwivedi, J. Non-Cryst. Solids. 289 (2001) 155.

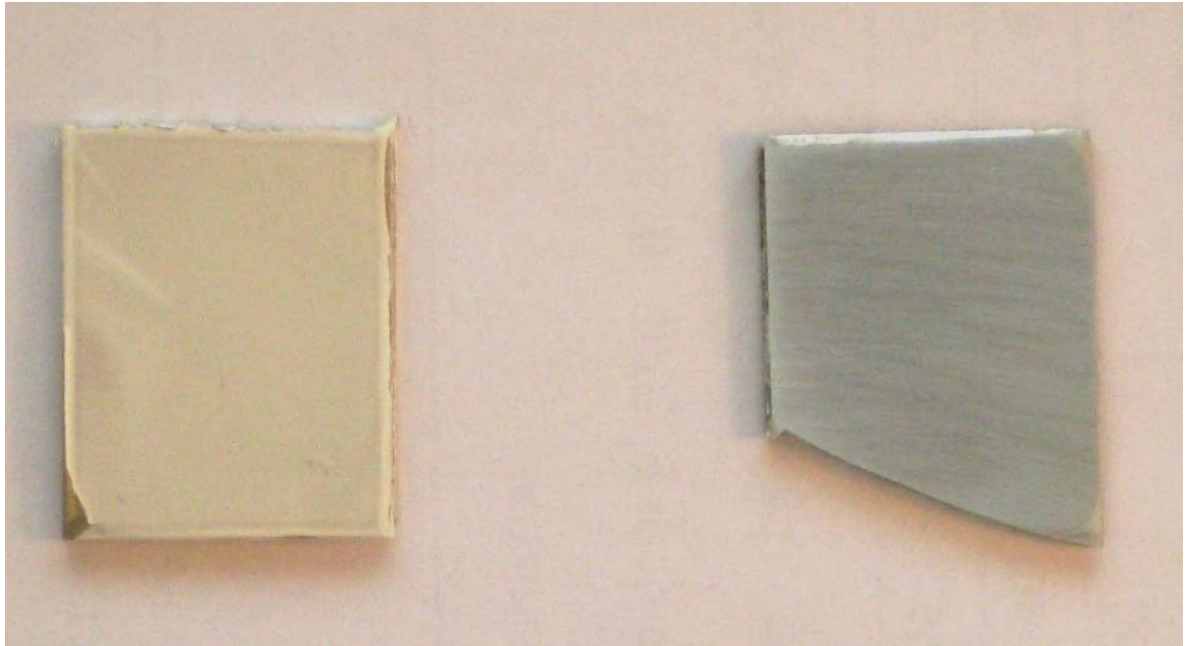
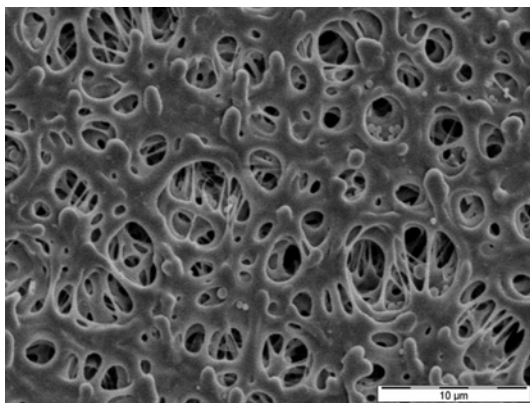
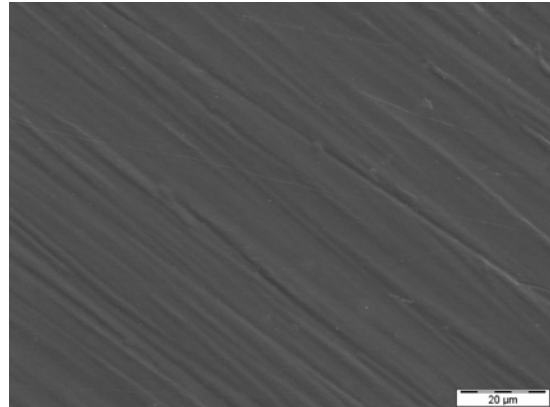


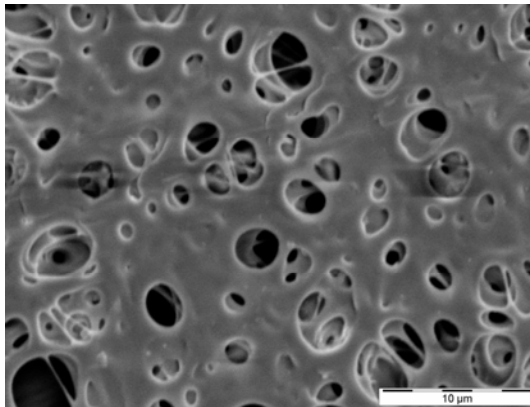
Figure1. In the left, a AZ31 sample spin coated with PEI/NMP (10/90) under room atmosphere. On the right a AZ31 sample spin coated with PEI/NMP (15/90) under N₂ atmosphere. Both coatings were prepared on grinded substrates.



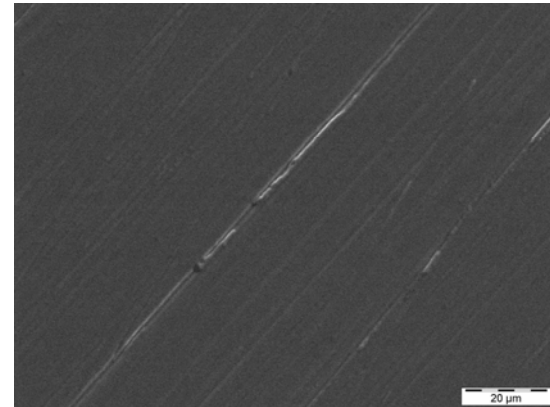
(a)



(b)

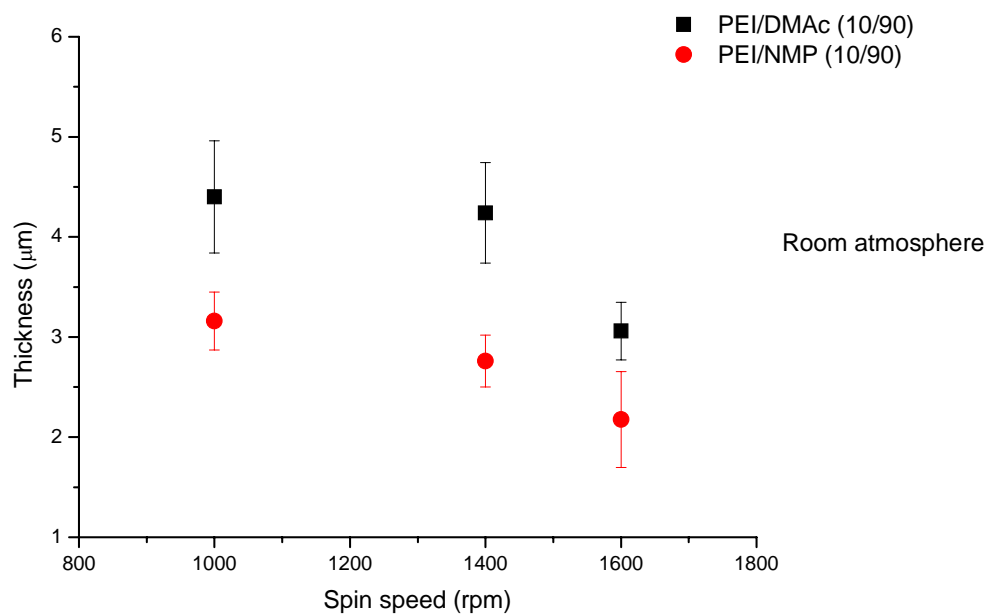


(c)

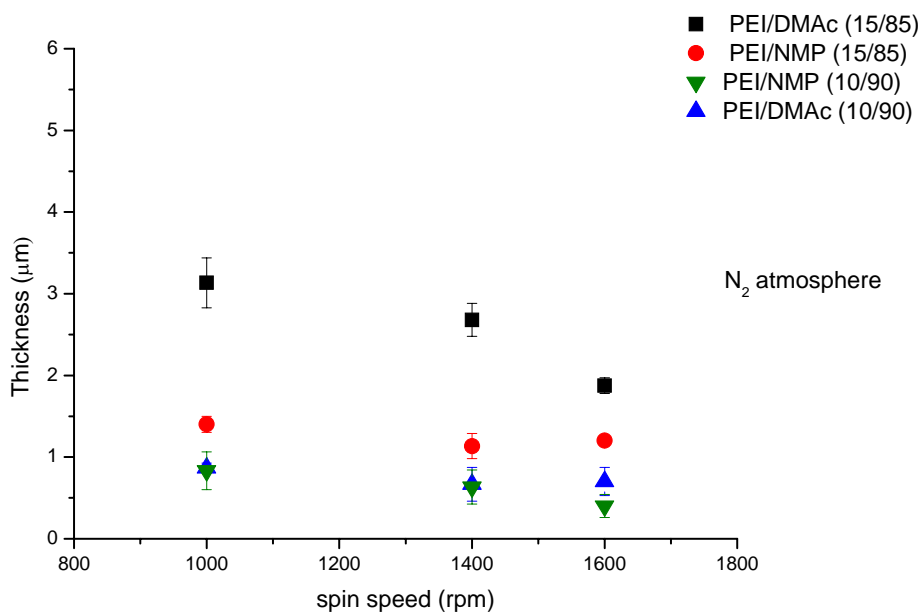


(d)

Figure2. SEM images of the spin coated samples prepared on grinded substrates. (a) and (b) are samples coated with PEI/DMAc (10/90) at room and N₂ atmosphere, respectively, and (c) and (d) are samples coated with PEI/NMP (10/90) at room and N₂ atmosphere, respectively.

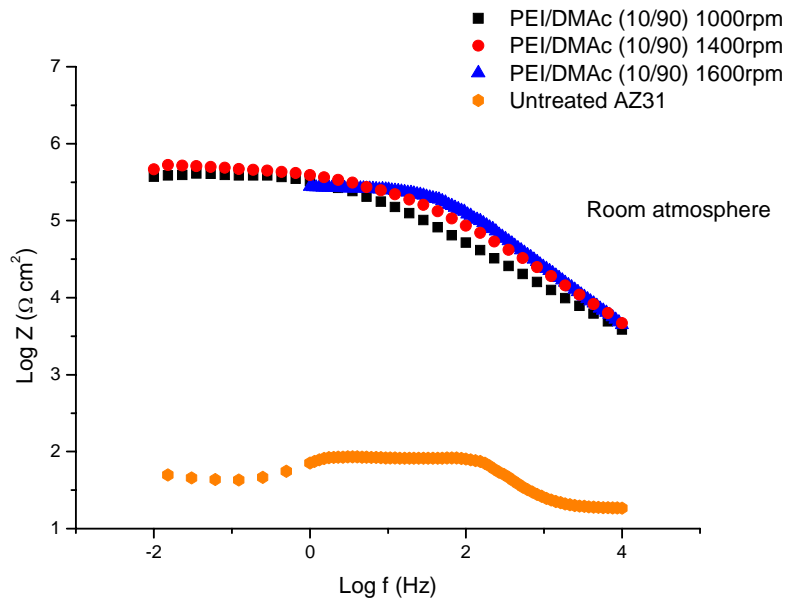


(a)

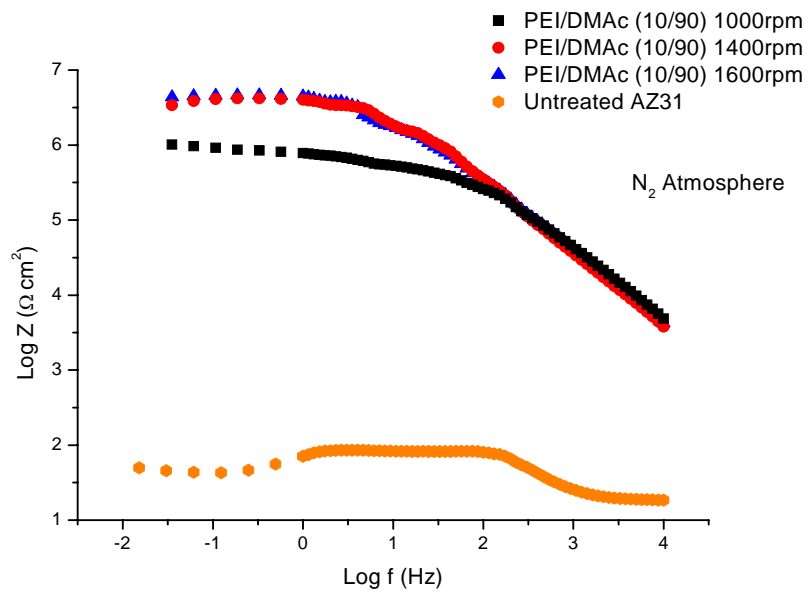


(b)

Figure 3. Thickness of the coatings as a function of spin speed: (a) Room atmosphere and (b) N₂ atmosphere

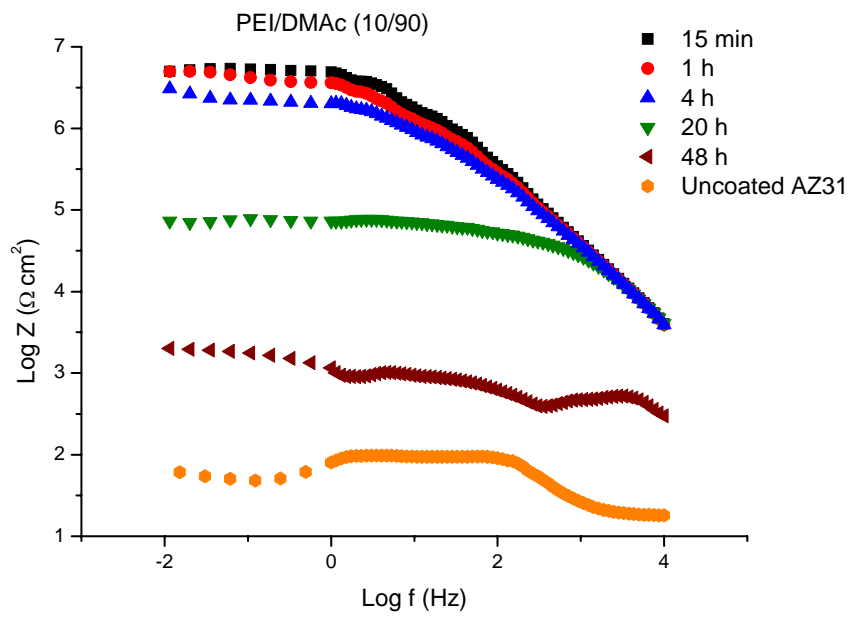


(a)

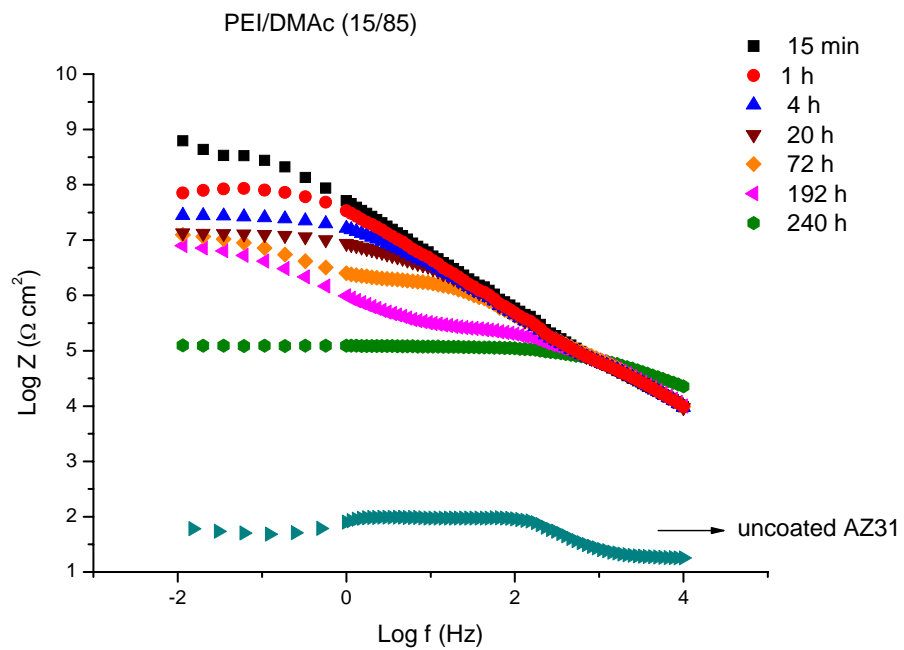


(b)

Figure 4. Impedance spectra of samples spin coated with PEI/DMAc (10/90) on grinded substrates, at different atmospheres and spin speeds. The measurements were performed after 15min of exposure to the 3.5% NaCl solution.

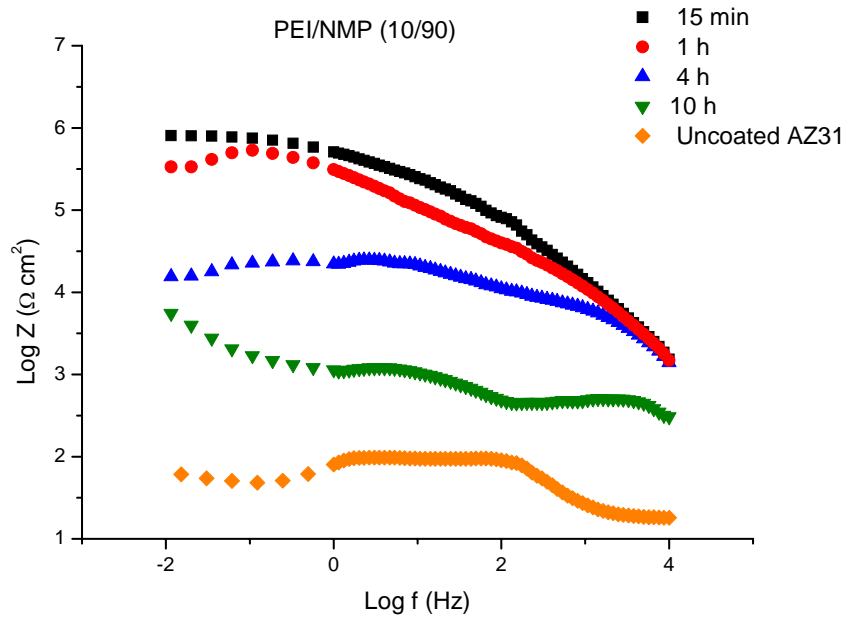


(a)

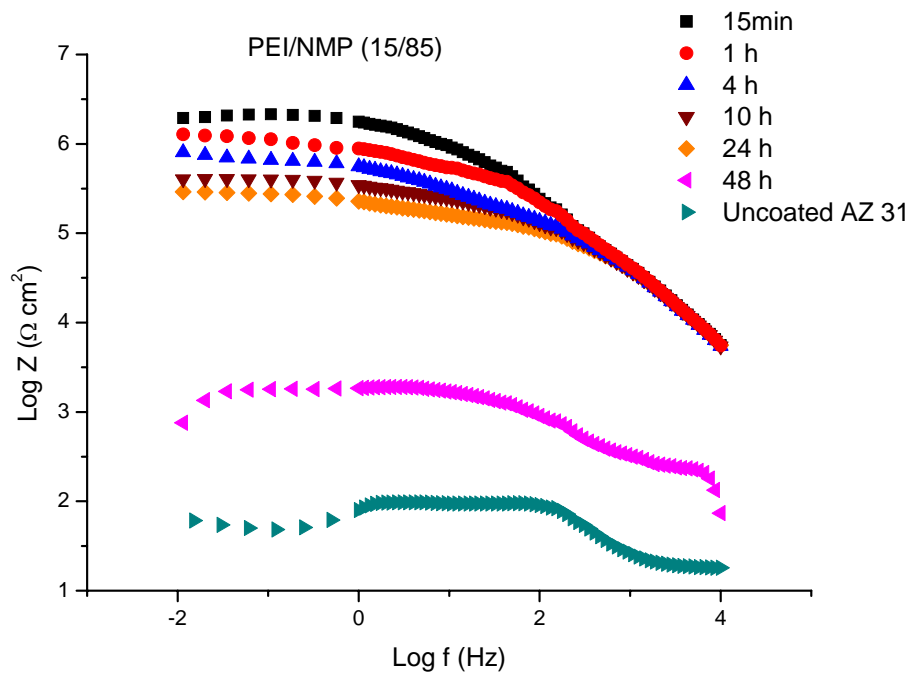


(b)

Figure 5. Impedance spectra of samples spin coated at 1400 rpm on grinded substrates using (a) PEI/DMAc (10/90) and (b) PEI/DMAc (15/85), under N_2 atmosphere at different exposure times to a 3.5% NaCl solution.

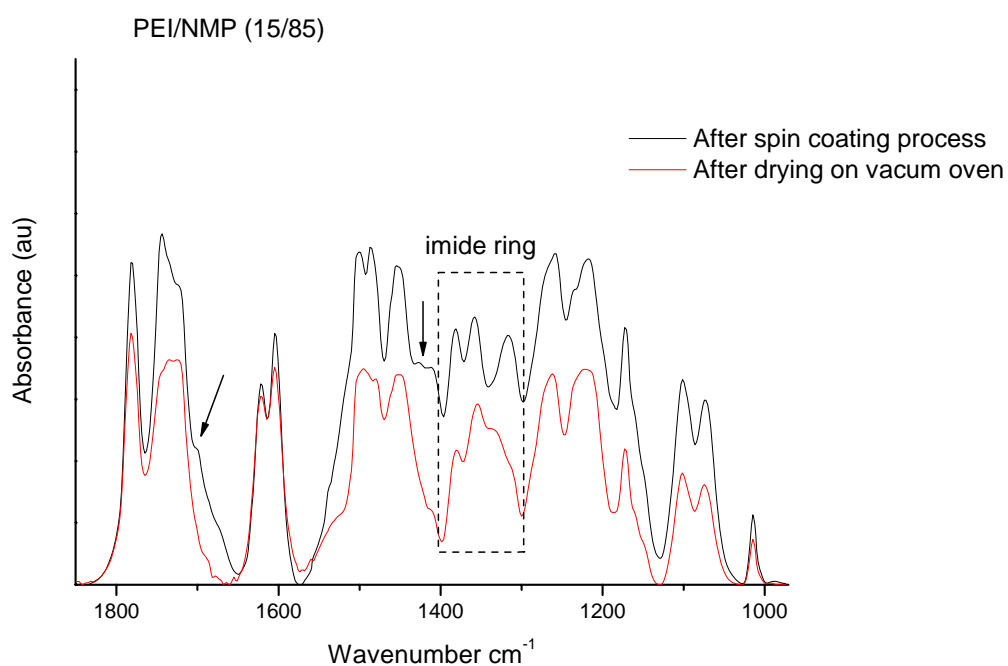


(a)

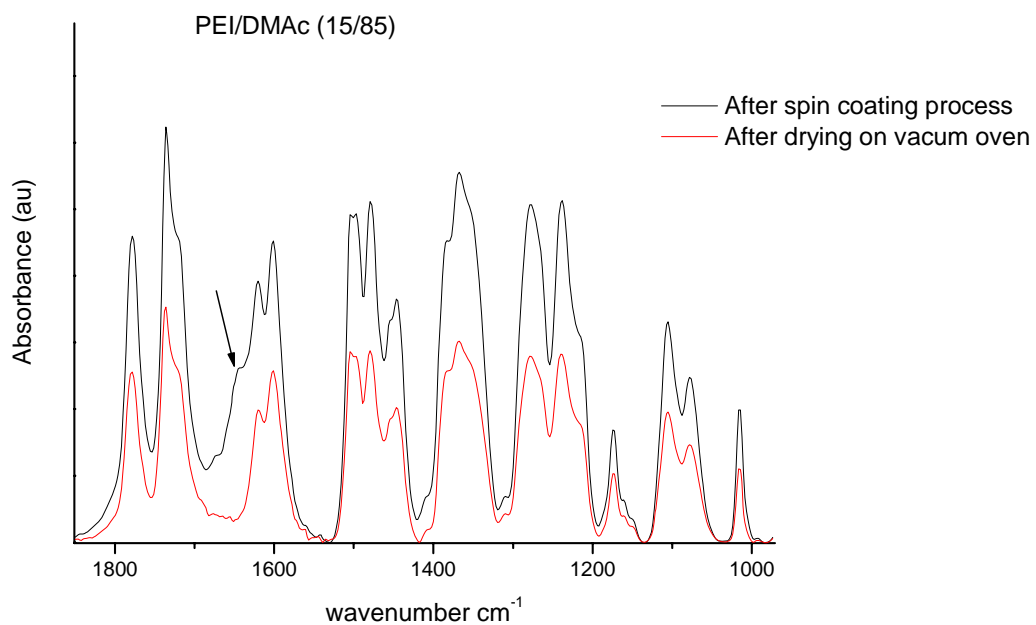


(b)

Figure 6. Impedance spectra of samples spin coated at 1400 rpm on grinded substrates using (a) PEI/NMP (10/90) and (b) PEI/NMP (15/85) under N_2 atmosphere at different exposure times to a 3.5% NaCl solution.

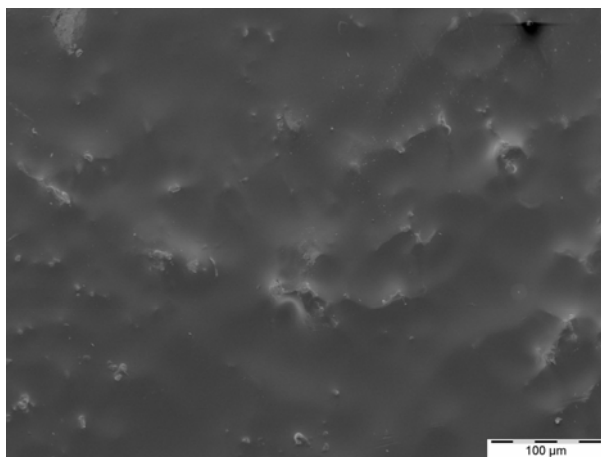


(a)

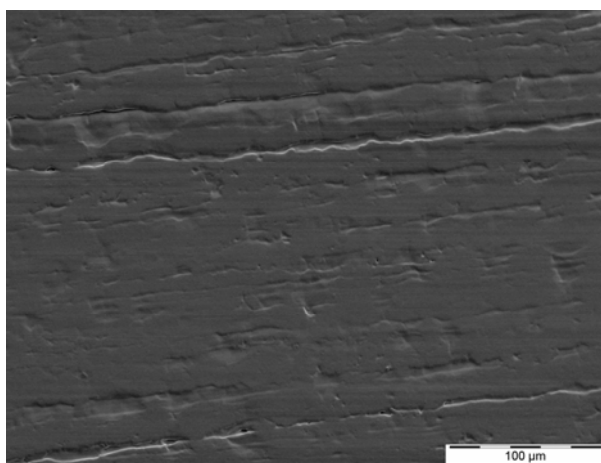


(b)

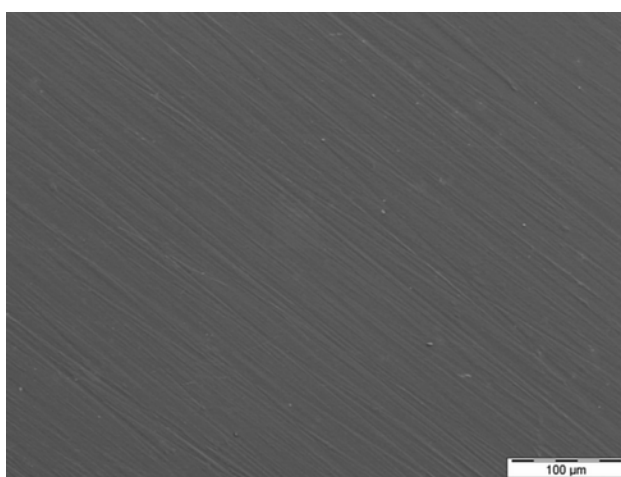
Figure 7. FTIR spectra of spin coated samples (grinded substrates) before and after drying in a vacuum oven at $135\text{ }^{\circ}\text{C}$ for 12h. The arrows in the figures indicate signals related to the solvents.



(a)



(b)



(c)

Figure 8. SEM images of samples spin coated at 1400 rpm using PEI/DMAc (15/85) on substrates treated with (a) 14HF, (b) acetic acid and (c) grinded.

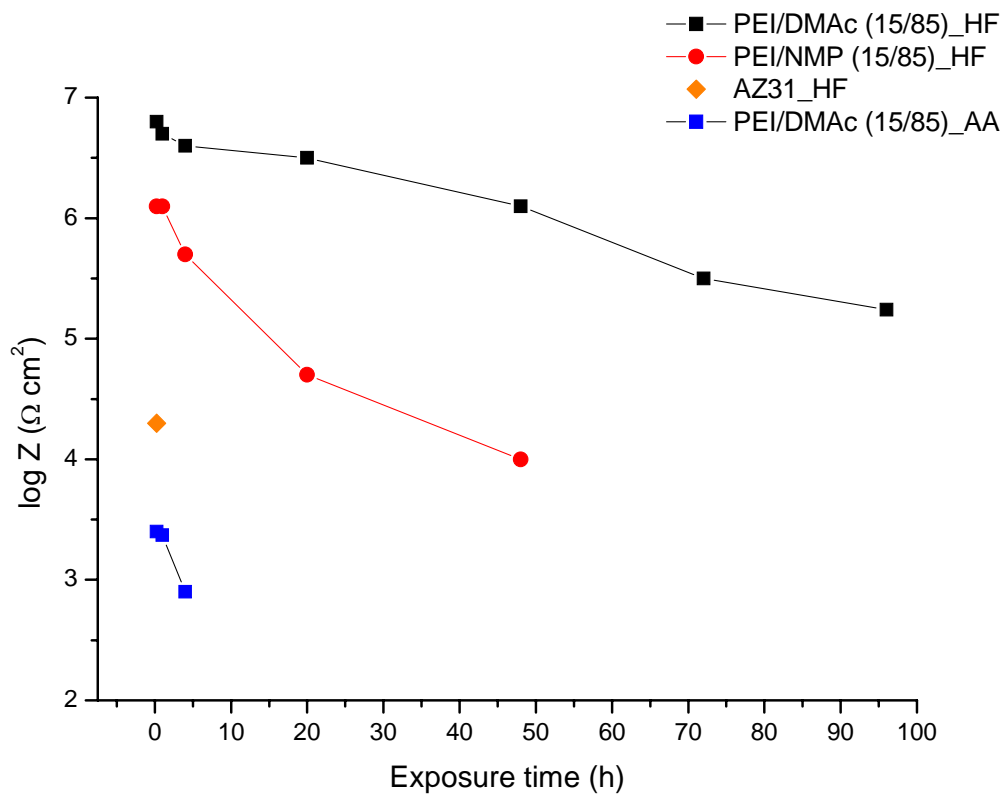
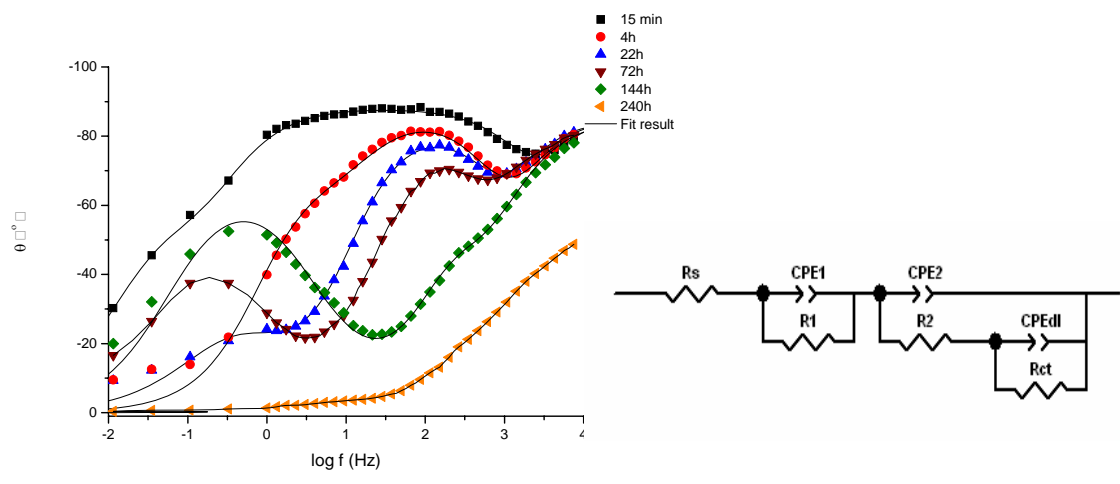
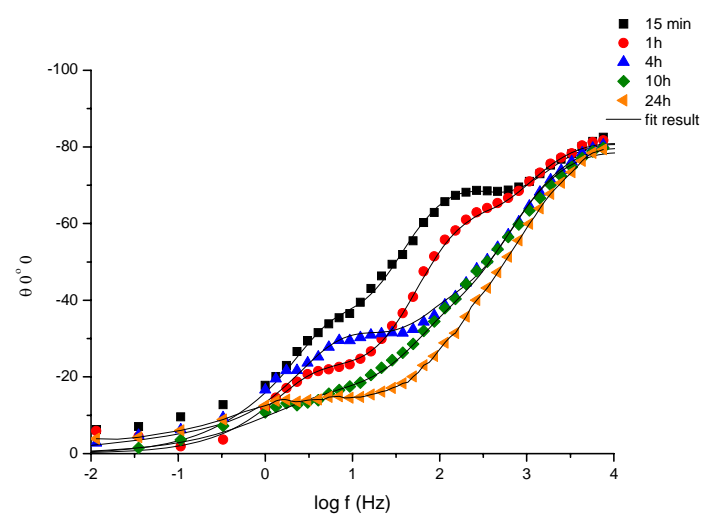


Figure 9. Low frequency (20 mHz) impedance of coated substrates pre-treated with HF and acetic acid (AA) at different exposure time to 3.5% NaCl solution.



(a)

(b)



(c)

Figure 10. Theta Bode plot of the samples coating with (a) PEI/DMAc (15/85) and (c) PEI/NMP (15/85) and the circuit used for the simulations of the results.

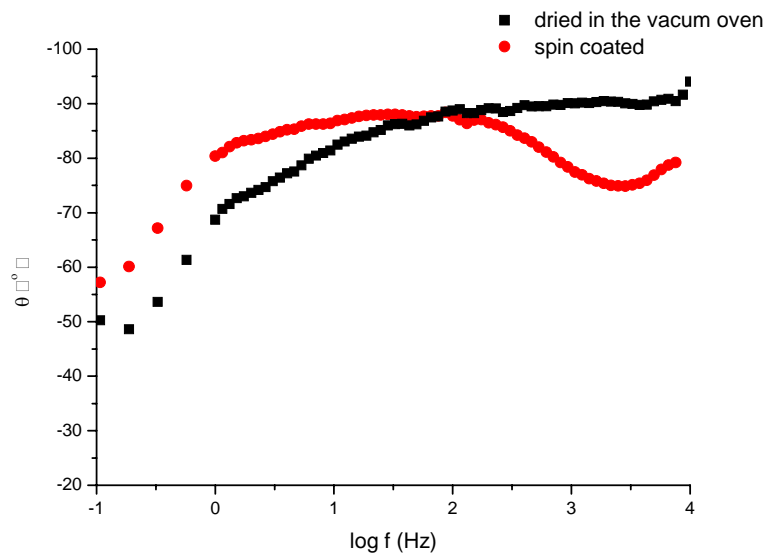
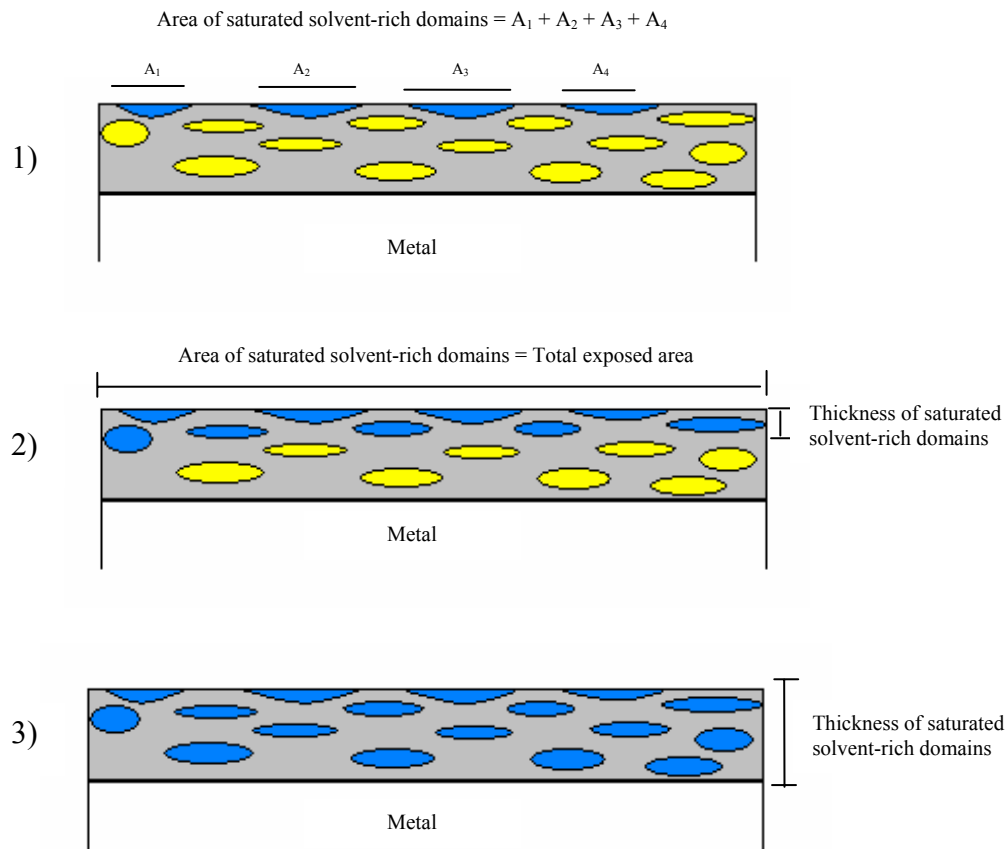


Figure 11. Theta Bode plot of spin coated and dried in a vacuum oven at 135 °C for 2h

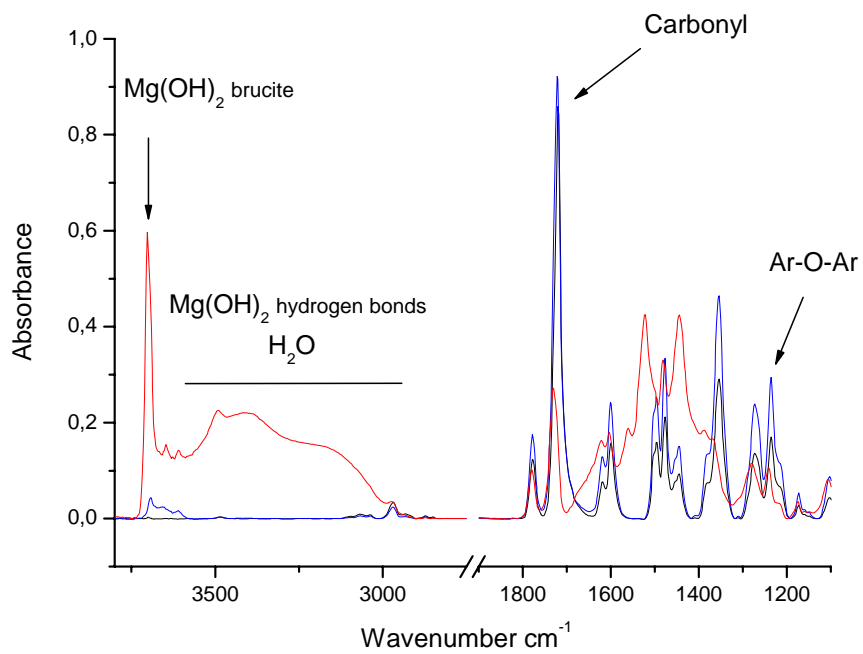


■ Saturated solvent-rich domains; ■ Solvent-rich domains

Figure12. Scheme of the electrolytes diffusion in the coating solvent-rich domains: 1) The electrolytes start entering in the coating saturating the solvent-rich domains on the coating surface. The area of saturated solvent-rich domains is smaller than the total exposed area. 2) The electrolytes diffuse in the coating saturating other solvent rich domains right beneath the coating surface. The area of saturated solvent-rich domains increases, becoming equal to the exposed area. 3) The electrolytes moves dip in the coating, saturating all the solvent-rich domains in the whole coating volume exposed to the solution. This results in an increase of the thickness of saturated solvent-rich domains.



(a)



(b)

Figure 13. (a) Microscopic image of a samples spin coated with PEI/DMAc (10/90) under N_2 atmosphere after 24h of exposure to 3.5% NaCl solution. (b) IR spectra of three distinct points of the sample surface.

Table 1. Chemical composition of the substrate

Sample	Mg (%) [*]	Al (%)	Zn (%)	Mn (%)	Fe (%)	Ni (%)	Cu (%)
AZ 31	95.70	3.23	0.823	0.225	0.008	0.001	0.001

^{*}In this table “%” is weight percentage.

Table 2. Properties of the solutions used

Solvent	Boiling point (°C)	Concentration (% wt.)	Viscosity (Pa s)
DMAc	165	10	0.043
		15	0.245
NMP	202	10	0.084
		15	0.620

Table3. Surface roughness

Substrate	Uncoated substrate roughness (μm)	Coated substrate roughness (μm)
Grinded	0.09 ± 0.01	0.03 ± 0.01
14HF-Treated	0.37 ± 0.02	0.26 ± 0.09
Acetic acid cleaned	2.21 ± 0.23	0.97 ± 0.09

Table 4. Values of the electronic circuit used in the simulation of the corrosion behaviour of coatings prepared using PEI/DMAc (15/85)

Time	CPE ₁		R ₁ (Ω cm ²)	CPE ₂		R ₂ (Ω cm ²)	CPE _{dl}		R _{dl} (Ω cm ²)
	T ₁ (Ω ⁻¹ cm ²)	P ₁		T ₂ (Ω ⁻¹ cm ²)	P ₂		T _{dl} (Ω ⁻¹ cm ²)	P _{dl}	
15 min	4.0 x 10 ⁻⁹	0.999	1.2 x 10 ⁴	3.0 x 10 ⁻⁹	0.980	3.0 x 10 ⁸	5 x 10 ⁻⁹	0.760	1.0 x 10 ⁹
3 h	4.0 x 10 ⁻⁹	0.976	3.0 x 10 ⁴	4.0 x 10 ⁻⁹	0.985	6.5 x 10 ⁶	8 x 10 ⁻⁹	0.800	2.0 x 10 ⁷
22 h	4.5 x 10 ⁻⁹	0.980	3.0 x 10 ⁴	4.6 x 10 ⁻⁹	0.96	4.0 x 10 ⁶	1.2 x 10 ⁻⁷	0.750	6.9 x 10 ⁶
72 h	6.6 x 10 ⁻⁹	0.930	5.0 x 10 ⁴	4.8 x 10 ⁻⁹	0.97	1.8 x 10 ⁶	1.8 x 10 ⁻⁷	0.798	1.2 x 10 ⁷
144 h	4.3 x 10 ⁻⁹	0.950	6.0 x 10 ⁴	8.0 x 10 ⁻⁹	0.95	2.4 x 10 ⁵	2.5 x 10 ⁻⁷	0.815	8.5 x 10 ⁶
240 h	-	-	-	2.2 x 10 ⁻⁸	0.678	1.2 x 10 ⁵	9.2 x 10 ⁻⁶	0.950	4000

Table 5. Values of the electronic circuit used in the simulation of the corrosion behaviour of coatings prepared using PEI/DMAc (15/85)

Time	CPE ₁		R ₁ (Ω cm ²)	CPE ₂		R ₂ (Ω cm ²)
	T ₁ (Ω ⁻¹ cm ²)	P ₁		T ₂ (Ω ⁻¹ cm ²)	P ₂	
15 min	9.8 x 10 ⁻⁹	0.980	2.0 x 10 ⁴	1.0 x 10 ⁻⁸	0.920	1 x 10 ⁶
1 h	9.8 x 10 ⁻⁹	0.978	2.6 x 10 ⁴	1.0 x 10 ⁻⁸	0.920	5 x 10 ⁵
4 h	9.5 x 10 ⁻⁹	0.920	6.5 x 10 ⁴	1.8 x 10 ⁻⁸	0.960	1.6 x 10 ⁵
10 h	9.7 x 10 ⁻⁹	0.920	6.8 x 10 ⁴	2.3 x 10 ⁻⁸	0.930	9.0 x 10 ⁴
24 h	6.5 x 10 ⁻⁹	0.950	6.0 x 10 ⁴	3.8 x 10 ⁻⁸	0.900	9.0 x 10 ⁴

Table 6 Adhesion test results

Sample	Adhesion strength (MPa)
PEI/DMAc (15/85)	2.00 ± 0.64
PEI/NMP (15/85)	2.25 ± 0.51